Title

Investigation of the Safety of Focused Ultrasound-Induced Blood-Brain Barrier Opening in a Natural Canine Model of Aging

Journal

Theranostics, 7(14)

ISSN

1838-7640

Authors

O'Reilly, Meaghan Anne

Jones, Ryan Matthew

Barrett, Edward

et al.

Publication Date

2017

DOI

10.7150/thno.20621

IVYSPRING INTERNATIONAL PUBLISHER

Theranostics

2017; 7(14): 3573-3584. doi: 10.7150/thno.20621

Research Paper

Investigation of the Safety of Focused Ultrasound-Induced Blood-Brain Barrier Opening in a Natural Canine Model of Aging

Meaghan Anne O'Reilly[1,2]✉, Ryan Matthew Jones[1,2], Edward Barrett[3], Anthony Schwab[4], Elizabeth Head[4] and Kullervo Hynynen[1,2,5]

1. Physical Sciences Platform, Sunnybrook Research Institute, Toronto, Ontario, Canada
2. Department of Medical Biophysics, University of Toronto, Toronto, Ontario, Canada
3. Lovelace Respiratory Research Institute, Albuquerque, New Mexico, USA
4. Sanders-Brown Center on Aging, University of Kentucky, Lexington, Kentucky, USA
5. Institute of Biomaterials and Biomedical Engineering, University of Toronto, Toronto, Ontario, Canada

✉ Corresponding author: Meaghan A. O'Reilly Sunnybrook Research Institute, 2075 Bayview Avenue, C736a, Toronto, Ontario, M4N 3M5, Canada; moreilly@sri.utoronto.ca; +1 416 480 5043

Received: 2017.04.17; Accepted: 2017.06.06; Published: 2017.08.22

Abstract

Rationale: Ultrasound-mediated opening of the Blood-Brain Barrier(BBB) has shown exciting potential for the treatment of Alzheimer's disease(AD). Studies in transgenic mouse models have shown that this approach can reduce plaque pathology and improve spatial memory. Before clinical translation can occur the safety of the method needs to be tested in a larger brain that allows lower frequencies be used to treat larger tissue volumes, simulating clinical situations. Here we investigate the safety of opening the BBB in half of the brain in a large aged animal model with naturally occurring amyloid deposits.

Methods: Aged dogs naturally accumulate plaques and show associated cognitive declines. Low-frequency ultrasound was used to open the BBB unilaterally in aged beagles (9-11yrs, n=10) in accordance with institutionally approved protocols. Animals received either a single treatment or four weekly treatments. Magnetic resonance imaging(MRI) was used to guide the treatments and assess the tissue effects. The animals underwent neurological testing during treatment follow-up, and a follow-up MRI exam 1 week following the final treatment.

Results: The permeability of the BBB was successfully increased in all animals (mean enhancement: 19±11% relative to untreated hemisphere). There was a single adverse event in the chronic treatment group that resolved within 24 hrs. Follow-up MRI showed the BBB to be intact with no evidence of tissue damage in all animals. Histological analysis showed comparable levels of microhemorrhage between the treated and control hemispheres in the prefrontal cortex (single/repeat treatment: 1.0±1.4 vs 0.4±0.5/5.2±1.8 vs. 4.0±2.0). No significant differences were observed in beta-amyloid load (single/repeat: p=0.31/p=0.98) although 3/5 animals in each group showed lower Aβ loads in the treated hemisphere.

Conclusion: Whole-hemisphere opening of the BBB was well tolerated in the aged large animal brain. The treatment volumes and frequencies used are clinically relevant and indicate safety for clinical translation. Further study is warranted to determine if FUS has positive effects on naturally occurring amyloid pathology.

Key words: Blood-Brain Barrier, Focused Ultrasound, Alzheimer's Disease

Introduction

Ultrasound-mediated opening of the Blood-Brain Barrier (BBB) is an area of increasing research due to its potential to significantly impact the treatment of brain disorders. The BBB regulates the passage of molecules from the vasculature to the brain parenchyma to maintain the brain environment, and in doing so prevents most intravenously-administered therapeutic agents from reaching the brain tissue in therapeutically relevant quantities [1]. One method to circumvent the BBB is to transiently open it using ultrasound [2]. When ultrasound interacts with intravenous diagnostic ultrasound contrast agents, micron-sized gas spheres known as 'microbubbles', it causes them to oscillate in the vasculature. The microbubbles stimulate the blood vessels in the brain and cause a transient opening lasting a few hours in length where therapeutics ranging in size from small molecule chemotherapeutics [3, 4, 5], to antibodies [6, 7], gene-delivery vectors [8, 9, 10] and stem cells [11] can be delivered. Investigations in non-human primates have demonstrated a good safety profile for this technique [12, 13, 14], and initial clinical investigations in brain tumor patients are underway in France [15] and Canada [16].

These methods also show promise in the treatment of Alzheimer's disease (AD). The first studies in mouse models of AD found that using ultrasound to deliver an anti-Amyloid β antibody resulted in a reduction of beta-amyloid (Aβ) plaque pathology 4 days post-treatment [6]. Interestingly, a later study showed that ultrasound opening of the BBB, in the absence of an externally administered therapeutic, also produced a positive effect on plaque load, presumably due to the treatment facilitating endogenous antibodies to reach the brain and/or activation of microglial cells [17]. Further, repeated opening of the BBB with ultrasound alone improves memory in two different transgenic mouse models of AD [18, 19].

Unlike mouse models of AD, which rely on genetic modification and overexpression [20], aged dogs naturally develop pathology and cognitive deficits [21]. Although the safety of this approach has been tested in large animals in the healthy brain [12, 13] safety in the aged, pathologic brain remains to be confirmed. It is unclear from the current literature if the aged brain will be as robust against the mechanical insult from the ultrasound and microbubbles. In addition, the larger brain of beagles allows clinically relevant low frequencies that penetrate the skull to be used in a larger skull cavity without significant impact from standing waves, as is case in the small skull of rodents [22]. Similarly, the tissue volume exposed in the dog brain can simulate the volumes needed to be exposed in clinical treatments. Therefore, this natural model allows investigations of BBB opening for the treatment of AD as a precursor to clinical investigations. In this study we investigate the safety of single and repeated BBB opening treatments in aged beagles (9-11yrs), which is an age at which most animals will have Aβ deposition. The results of these treatments and a two week follow-up period are reported.

Materials and Methods

Study Design

The objective of this study was to test the safety of ultrasound-mediated BBB opening in the aged brain with clinically relevant exposure conditions and treatment volumes. Aged beagle dogs (n=10, 9-11yrs, 10.1-13.8kg) with naturally occurring amyloid pathology were used, in accordance with institutionally approved protocols (Sunnybrook Research Institute animal care committee) and in keeping with the Canadian Council on Animal Care guidelines on the care and use of laboratory animals. The animals were divided into two groups (each n=5), the first receiving a single treatment, and the second group receiving weekly treatments for four weeks. The effects were monitored using MRI, neurological testing and histological analysis.

Animal Preparation

The animals had a range of underlying medical conditions, including cancer, and this was an end-of-life study prior to euthanasia. Anesthesia was induced with acepromazine (0.2mg/kg, intramuscular). The animals were intubated and anesthesia was maintained using oxygen and 2% isofluorane. The carrier gas was changed to medical air 10 mins prior to the first treatment sonication. The cephalic or saphenous vein was catheterized using a 22-20G angiocatheter. The hair on the head was removed using an electric razor and depilatory cream.

The animals were mechanically ventilated during the treatment and imaging procedures, and the heart rate was monitored using a pulse oximeter. While anesthetized, the body temperature was maintained using a circulating water blanket and was regularly checked using a rectal thermometer.

The animals were assigned to one of two groups. In the first group the animals received a single ultrasound treatment and then were followed for two weeks. After no significant adverse effects were observed following the single treatment, a second group of animals received treatments weekly for 4 weeks, followed by a 2 week follow-up period.

Ultrasound Exposures

For the treatments, the animals were positioned supine above an MRI-compatible three-axis positioning system, operationally similar to that described by Ellens et al [23], that would mechanically position the ultrasound focus by moving a single-element, fixed focus transducer. The experimental setup is illustrated in Fig.1. The ultrasound was generated by an in-house assembled, spherically curved, lead zirconate titanate (PZT) transducer (PZT from DeL Piezo Specialties, LLC, West Palm Beach, Florida), with a 75 mm diameter, focal-number 0.8 and fundamental frequency, f_0 = 0.28 MHz. The transducer was matched to 50 Ω, 0° at its fundamental frequency using an external matching circuit, and driven using a function generator (33220A; Agilent, Santa Clara, California) and an RF amplifier (NP2519; NP Technology, Newbury Park, California). Sonications were applied transcranially. All pressure estimates reported in this paper are based on the calibration of the transducer in water using a fiber-optic hydrophone (Precision Acoustics, Ltd, UK) and are not de-rated for transmission through the skull-bone due to the wide variation in cranial geometry, and hence insertion loss, between animals (Fig.2). The measured dimensions of the transducer focal spot (full-width-at-half-maximum pressure) were 6.5 mm in the transverse direction, and 40 mm axially. The insertion loss at 280 kHz was measured in 4 of the skull caps following tissue harvest using the fiber-optic hydrophone system. Measurements of the focal pressure amplitude were made at a total of 20 locations across the 4 skulls and a mean (± S.D.) transmission of 53 ± 15% was measured.

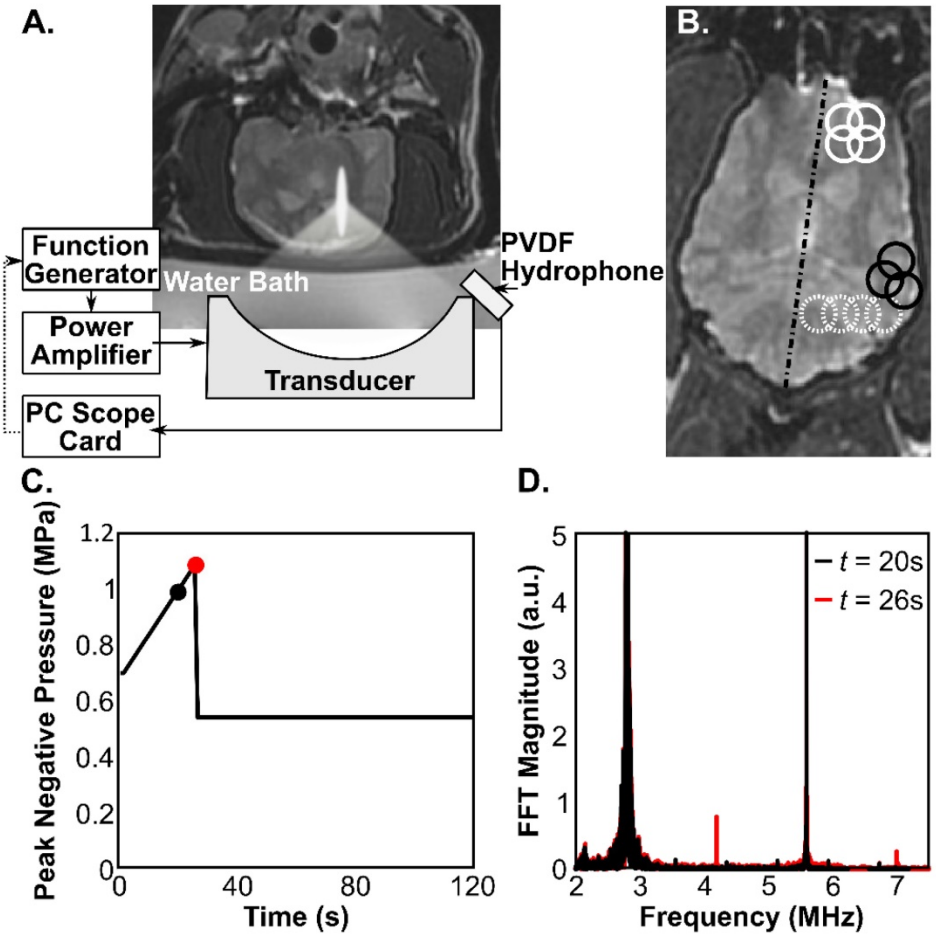

Fig.1. A) Experimental setup. A coronal T_2-weighted MR image shows the orientation of the transducer with respect to the subject. B) Example sonication grids overlaid on an axial T_2-weighted MR image. Solid white circles: 2x2 grid with 4.5 mm spacing, Dashed white circles: 1x4 line with 4.5 mm spacing, Solid black circles: reduced, 3 point grid with 4.5 mm spacing to fit the brain geometry at the edges of the brain cavity. The dashed black line indicates the brain midline. The diameter of the circles is the approximate FWHM of the focal spot. C) Example pressure vs. time curve for one sonication focus, showing the peak negative pressure (free-field) for each burst of ultrasound. The black and red circles correspond to timepoints below (black) and at (red) the threshold for detecting ultraharmonic microbubble behavior. The spectra corresponding to these two bursts are overlaid in (D), where signals at 0.42 and 0.7 MHz (1.5f_0 and 2.5f_0) are seen in the red trace.

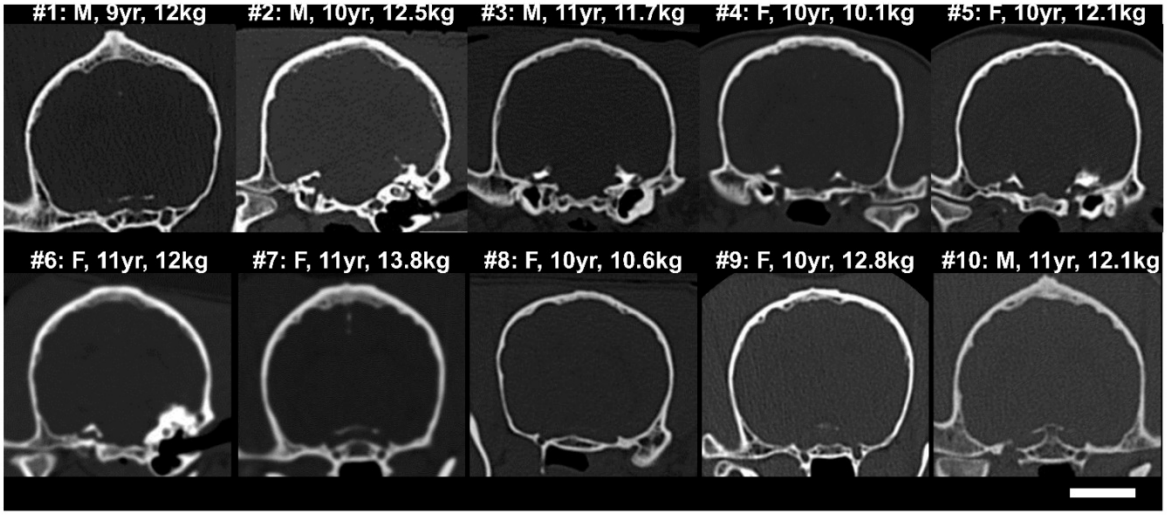

Fig.2. CT skull cross-sections (coronal) from (top) the 5 subjects in the acute treatment group, and (bottom) the 5 subjects in the repeat treatment group. The sex, age and weight of the subjects at the time of treatment are shown. The scale bar is 2 cm.

Definity microbubbles (Lantheus Medical Imaging, N. Billerica, MA, USA) were used to potentiate the BBB opening effect and were injected simultaneously with the start of the ultrasound exposure at a dose of 0.02 ml/kg per injection. The mechanical positioning system used is limited in the speed of travel between treatment points. For the 10 ms ultrasound bursts used in this study, the positioner could rapidly move to and treat up to 4 points at 4.5 mm spacing within 1 second, allowing for a 1 Hz pulse repetition frequency (PRF) per point. A larger number of focal points could be treated in one sonication (one bubble injection) by reducing the PRF to allow more time to cycle through the targets. In the first animal the sonications were 3 minutes in length, and consisted of 10 ms bursts at a 0.33 Hz, per point PRF, for a total of 60 bursts per target. The 0.33 Hz PRF allowed 3 seconds for the positioning system to cycle through 9 targets in a 3x3 grid with 4 mm spacing. The sonication pressure was fixed for the sonication and ranged from 0.8-1 MPa (free-field estimate). In the remaining 9 animals the treatment pressures were modulated during the sonications, using the control scheme reported in [24], which is also briefly described in the following: Microbubble emissions during the sonications were captured to PC with a sampling rate of 20 MHz and an 11 ms capture length using a wideband, PVDF receiver [25] connected to a 14 Bit PCI digitizer (ATS460, Alazar Tech, Pointe Claire, Quebec). After each burst the frequency content of the data was analyzed. Starting at a value of 0.6-1 MPa, the pressure was increased by 0.016 MPa for each subsequent burst until ultraharmonic microbubble emissions ($1.5f_0$ or $2.5f_0$) were detected. Prior work in rats has shown that these emissions precede the appearance of wideband emissions indicating inertial cavitation, and can thus be used as an internal calibration point to stay below the threshold for tissue damage [24]. This means that each sonication point received an acoustic exposure based on the acoustic emissions detected, thus minimizing the variations caused by skull thickness and angle of incidence [26, 27, 28]. The peak pressure (mean ± S.D.) reached in these sonications was 1.2 ± 0.3 MPa. Following detection of the ultraharmonic signals the pressure was decreased by 50 % and maintained for the remainder of the sonication (Fig.1C, D). The actively controlled sonications were performed at a 1Hz PRF for a total of 2 minutes (120 bursts per target) using 2 x 2 or 1 x 4 interleaved target grids with 4.5 mm spacing (Fig.1B). At the edges of the brain, some sonications were reduced to 3 or 2 points to fill the remaining space without overlapping previous sonications. For both sonication schemes the sonications were repeated with new targets until the entire hemisphere had been treated. A minimum of 5 minutes was allowed between sonications for the microbubbles from the previous injection to clear. The total number of sonications with separate microbubble injections varied between 7 and 13 per treatment with a mean value of 9 ± 2. The total number of foci sonicated in this study was 920. This value is the total number of focal spots required to cover the treated hemisphere, summed over all animals and all treatments.

CT and MRI Imaging

All animals were imaged in an x-ray computed tomography (CT) scanner (Aquilon ONE, Toshiba America Medical Systems, Inc., Tustin, California). The field of view was adjusted slightly based on the animal size and was reconstructed using a 512x 512

image matrix, resulting in voxel dimensions that varied slightly between animals but were at most 0.35 x 0.35 x 1 mm^3. The CT images were captured to allow better visualization of the skull geometry and porosity to anticipate potential issues with sound transmission during the treatments.

The MRI parameters used are summarized in Table 1. All treatments were performed under MRI-guidance at 3T (Signa MR750, GE Healthcare, Milwaukee, Wisconsin). Baseline T1 and T2 weighted images were obtained and are shown for group 1 in Fig.3. Contrast-enhanced (CE) T1 weighted imaging (0.1 ml/kg Gadovist) was used to assess the integrity of the BBB post-treatment, and post-treatment T2 and T2* images were used to identify edema or hemorrhage. Follow-up MR imaging was performed one week following the final treatment, using CE-T1, T2 and T2* weighted imaging. The follow-up imaging was performed on the same MRI scanner used during the treatments, except in one case where the system was unavailable and an alternate 3T platform was used (MAGNETOM Prisma, Siemens Healthcare, Erlangen, Germany).

Table 1. MRI parameters

	GE			Siemens		
Parameter	**T1**	**T2**	**T2***	**T1**	**T2**	**T2***
Sequence type	Fast spin echo	Fast spin echo	3D gradient echo	Turbo spin echo	Turbo spin echo	3D gradient echo
Echo time (ms)	14.52	58.08	3.3348	16	79	15
Repetition time (ms)	500	3000	8.108	500	3000	27
Echo train length	4	4	1	4	8	1
Averages	3	1	1	2	2	2
Field of view (cm)	14x14	14x14	14x14	14x14	14x14	14x14
Matrix	256x256	256x256	256x256	128x128	128x128	128x128
Slice thickness (mm)	1.5	1.5	1	1.5	1.5	1

Neurological Testing

The animals were subjected to a neurological exam 24 hrs after the ultrasound treatment (Group 1) or daily beginning 72 hrs before the first treatment and continuing until the study end (Group 2). The exam included observations of general mental status, posture and movement, as well as cranial nerve function and postural reactions. The complete neurological exam criteria are included in Table 2. The testing did not assign a numeric score as the criteria were assessed as pass/fail, with animals either having a consistent response with their prior health history or baseline data, or an abnormal response.

Histological Processing and Analysis

Two weeks following the final treatment in each group, the animals were deeply anesthetized and sacrificed using approved animal protocols. Brains were fixed in 4% paraformaldehyde for 48-72 hrs prior to transfer to phosphate buffered saline (pH 7.4) and storage at 4^0C. The prefrontal cortex was dissected from both the left and right side for all animals and sectioned at 50μm using a vibratome. This is typically the brain region affected earliest by Aβ deposition in beagles [29]. Tissue was stained for Aβ plaques using previously published immunohistochemical methods [30] with 6E10 antibody (Aβ1-16, Covance, Dedham, MA; 1:3000, mouse monoclonal) after the tissue was pre-treated in 90% formic acid for 4 min [31]. Adjacent sections were used for microglial immunostaining with the IBA-1 antibody (for possible inflammation, Wako Chemicals USA, Richmond, VA, 1:800, rabbit polyclonal) and Prussian blue staining to identify microhemorrhages using previously published protocols [32].

Aβ and IBA-1 immunostained slides were imaged using an Aperio ScanScope XT digital slidescanner at 40x magnification to create a high resolution digital image. The Aperio positive pixel count algorithm (version 9) was used to quantify specific staining in 10-600x600μm^2 fields. Quantification of Prussian blue staining was by counting microhemorrhages in each tissue section using a 20X objective and counting within 10 fields/section. Prussian blue labeling within 2 cell diameters of a blood vessel was considered a microhemorrhage.

Statistical Analysis

Although the sample size was small, a repeated t-test was used to compare the left and right hemisphere Aβ loads in the two treatment groups and in all 10 animals.

Results

The treatment parameters, including the number of microbubble doses and sonication foci targeted, as well as a summary of adverse events, are summarized on a per-animal basis in Table 3.

CT and MRI findings

CT images from the 10 animals showing coronal cross-sections of the skull bone are shown in Fig.2. It can be seen that the bone thickness and geometry varied substantially between animals. The dog skulls had a mean thickness (± S.D.) of 3.2 ± 1.1 mm (maximum 9.2 mm), estimated over 25 locations/skull, and a mean density (± S.D.) of 2172 ± 509 kg/m^3 (maximum 3691 kg/m^3). The brain cavities of the 10 dog skulls were measured to be 42.5 ± 1.6 mm deep, 52.4 ± 1.5 mm wide and 71.2 ± 3.6 mm long.

Table 2. Neurological testing template

Mental Status:	*Categorize overall mental status:* BAR *(bright, alert, responsive)* / QAR *(quiet, alert responsive)* / Stuporous *(only responsive to painful stimuli)* / Comatose *(non-responsive)*
Body Posture:	*Describe any abnormal body posture:* Head Tilt (L/R) / Head Turn (L/R) / Circling (L/R)
Gait:	*Describe any abnormalities in gait, specifying involved limb(s):* Paresis *(weakness of voluntary movement)* / Paralysis *(absence of voluntary movement)* / Lameness *(uneven gait caused by pain or stiffness)*
Ataxia:	*Describe any irregular or inconsistent movements:* Proprioceptive *(scuffing or dragging the paws on the ground, knuckling over, crossing over, or interference)* / Vestibular *(unable to walk in a straight line)* / Cerebellar *(undershooting or overshooting of intended position with paw)*
CRANIAL NERVES	
Pupil (CN III):	*Record size, symmetry and shape of pupils*
Menace (CN II/VII):	*Make a threatening gesture at the eye to induce a blink*
PLR (CN II/III):	*Shine a light into one eye and look for pupil constriction in both eyes*
Strabismus (CN III/IV/VI):	*Eyes are not aligned due to lack of coordination between the extraocular muscles*
Corneal Reflex (CN V/VI):	*Gently touch the cornea with a moist soft cotton swab to induce global retraction*
Jaw Tone (CN V):	*Observe and palpate muscles of mastication for any swelling, atrophy, or asymmetry. Animal many not be able to close mouth if there is bilateral weakness*
Maxillary & Mandibular (CN V):	*Gently pinch the lips and look for retraction of the lips. Also, touch the medial nasal mucosa with a hemostat and look for retraction of the head*
Palpebral (CN V/VII)	*Gently touch the medial & lateral canthus of the eye to induce a blink response*
Nystagmus (CN VIII):	*Observe the eyes for nystagmus while moving the head slowly laterally in both directions, and up and down.*
POSTURAL REACTIONS	
Proprioceptive positioning:	*With the animal standing, turn over one paw and place the back of the paw on the floor. The animal should quickly correct the position of the paw.*
Hopping:	*Hold the animal so that all of its weight is supported by one limb and move the animal forward or laterally. The animal should make a quick, smooth step in response*
Wheelbarrow:	*Lift the hind limbs off the ground and gently push the animal forward. The animal should make alternating steps with its forelimbs.*
Extensor Postural Thrust:	*Hold the animal leaving just the hind limbs on the ground and gently push the animal backward. The animals should make coordinated steps backwards.*
Placing Reactions:	*Cover the animal's eyes and move the animal towards the edge of a table. The animal should place their paws on the table as soon as there is contact*

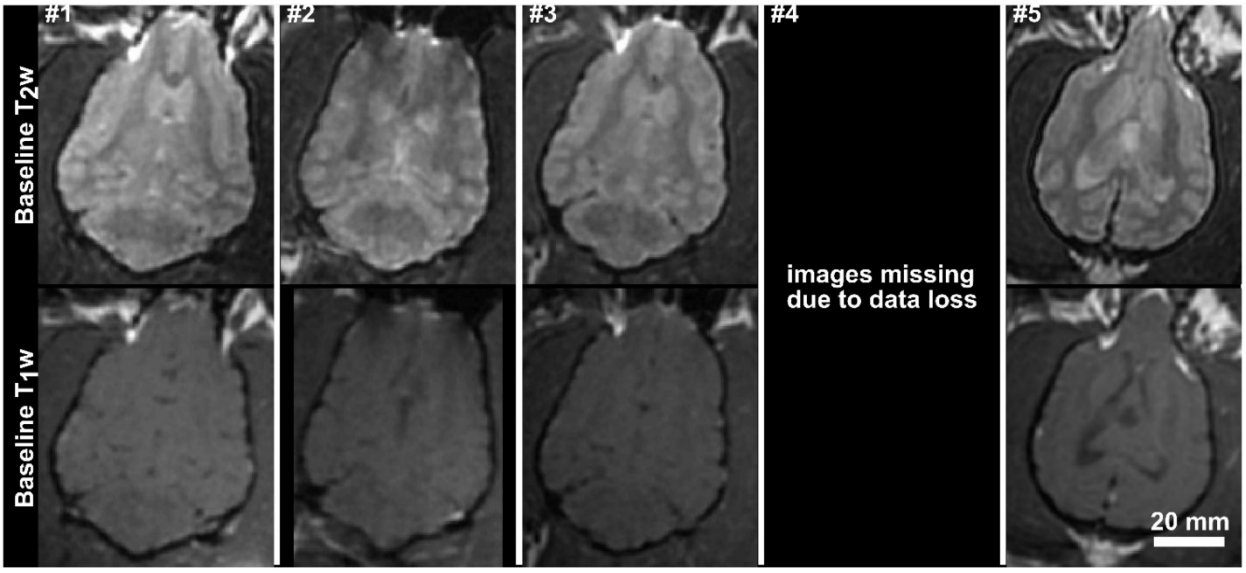

Fig.3. Baseline T_1-weighted and T_2-weighted axial MR images for the 5 subjects in the acute treatment group. The images for subjects 1, 2 and 3 have been resliced from oblique image stacks. The scale bar is 2 cm.

To compare, the average thickness and density of the supraorbital region of 8 ex vivo human skulls (4 skull caps and 4 full skulls) in our laboratory was extracted from existing CT data. The human skulls were found to be approximately twice as thick (6.4 ± 1.8 mm, maximum 20.3 mm) and were similar but not quite as dense (1900 ± 373 kg/m^3, maximum 2975 kg/m^3) as the dog skulls. The brain cavities of the 4 full human skulls were 108.4 ± 4.2 mm deep, 137.2 ± 9.9 mm wide and 162.3 ± 5.2 mm long. Despite the bone morphology, the permeability of the BBB was successfully increased unilaterally using transcranial ultrasound (Fig.4). A mean enhancement of 19 ± 11% was observed across all treatments relative to the untreated hemisphere. Heterogeneous patterns of enhancement were observed in all animals.

Enhancement was not seen in the white matter tracts, which is consistent with investigations of BBB opening in primates [12] and can be attributed to the fact that white matter is poorly vascularized resulting in limited signal from the extravasated contrast agent. The post-treatment images for animal #4 are missing due to a data loss, but the degree of enhancement and the heterogeneity of the enhancement were in keeping with the other four animals in the single treatment group. The mean intensity across the entire hemisphere relative to the control hemisphere is shown for each treatment and follow-up in Fig.5. These are expressed as (1-mean_intensity$_{treated}$/ mean_intensity$_{untreated}$)*100%, and thus negative values can occur when the mean intensity of the treated side is lower than the control side. Also shown are the mean intensity in an unsonicated region (usually in the olfactory bulb or cerebellum) of the treated hemisphere relative to the same region on the treated side. This control region is included because in some cases there were substantial differences in the intensity of the MR images resulting from the positioning of the surface coil. For example, the coil placement during the follow-up imaging of animal #6 resulted in an intensity gradient left to right across the brain. Examining only the treated vs. untreated intensities makes it appear that there is enhancement in the treated region. Examining the unsonicated control region, it can be seen that the higher intensity in the left hemisphere is unrelated to the treatment region. The heterogeneity of the BBB opening is reflected by the large standard deviations in the treated hemispheres.

At one week post treatment, the BBB was fully intact in all animals and there were no indications of damage to the brain tissue on the T2 and T2* weighted images. In the first animal, thermal damage was seen in the overlying muscle at follow-up and was confirmed at necropsy. This was attributed to a technical error that saw higher pressure exposures (>2 MPa), interleaved at several locations, applied in the absence of injected microbubbles. Because there were no bubbles in circulation, there was no associated damage to the brain tissue observable by MRI or in histology. Thermal damage was not seen in any of the remaining animals, where the sonications were correctly performed.

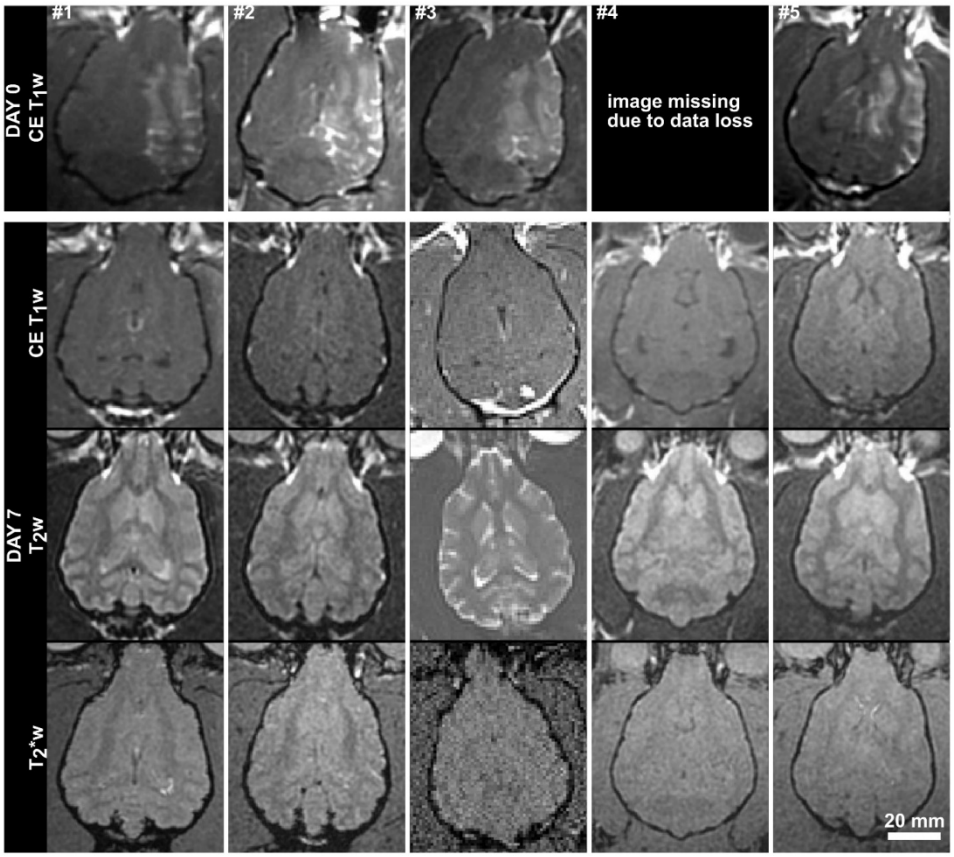

Fig.4. MR (axial) images from the 5 subjects in the acute treatment group acquired immediately post-treatment and at 7 days post-treatment. Contrast-enhanced (CE) T1w images are shown on Day 0, and CE-T1w, T2w and T2* weighted images are shown for Day 7. The Day 0 image for subject #1 has been resliced from an oblique plane. The Day 7 images for subject #3 were acquired using a different MRI scanner (Siemens Prisma). The scale bar is 2 cm.

Neurological testing and adverse events

All animals were alert and responsive following the treatments. Gait and postural reactions were consistent with baseline testing or the animals' prior health histories, and cranial nerve testing was normal in all animals.

One minor adverse event was observed. 24 hr following the second treatment, the first animal in the chronic treatment group had bloody urine and was vomiting. In consultation with the institutional veterinarian this animal was given IV fluids and started on oral antibiotics as a precaution. The symptoms were resolved 24 hours following. As the first animal in the repeat treatment group, the treatment times for this animal were longer as the treatment process had not been optimized. The prolonged anesthesia time and the number of MRI contrast agent injections were thought to have contributed to the adverse reaction. For the remaining treatments the MR imaging protocols on treatment days were optimized to reduce the total treatment time, and hence anesthetic time, and MRI contrast agent injections were limited to two per treatment. No adverse events were observed following these modifications.

Tissue analysis

Table 3 details the results of the tissue analysis on a per-animal basis. There were no statistically significant reductions in Aβ load in the left hemisphere as compared to the right hemisphere in the single treatment group ($t(4)=1.17$ $p=0.31$) and loads were significant correlated across hemispheres ($r=0.88$ $p=0.048$). However, 3/5 dogs showed lower left prefrontal cortex loads (Fig.6 A,B) relative to the untreated right prefrontal cortex. In the multiple treatment condition, a similar result was observed with no statistically significant decreases in Aβ ($t(4)=0.12$ $p=0.98$) but the two hemispheres were not correlated ($r=0.03$ $p=0.96$). In this group, 3/5 dogs also showed lower left prefrontal cortex Aβ compared to right prefrontal cortex (Fig.6 C, D) but 2/5 animals did not show any clear reduction of Aβ (Fig. 6 E, F). . IBA-1 loads (Fig.7, Table 3) and the number of microhemorrhages (Table 3) in the prefrontal cortex were similar across hemispheres in both groups. In the single treatment group, the mean number of microhemorrhages in the treated side was 1.0 ± 1.4, compared with 0.4 ± 0.5 on the untreated side. In the multiple treatment condition, an average of 5.2 ± 1.8 microhemorrhages were detected in on the treated size vs. 4.0 ± 2.0 on the contralateral size. Statistical analysis was not performed due to the extremely low counts.

Table 3. Summary of treatment parameters and outcomes. (A - Fixed pressure, 0.33 Hz PRF, 3 minutes, 9 interleaved foci per sonication at 4 mm spacing; B - Actively controlled pressure, 1 Hz PRF, 2 minutes, up to 4 interleaved foci per sonication at 4.5 mm spacing; * Variations in the number of injections and sonication spots per treatment for the repeated treatments is a result of variables such as animal positioning (e.g. a different angle of the head requiring targeting at two different depths to ensure complete coverage of the brain) and incomplete sonications (e.g. software crash halting the treatment mid-sonication and requiring a second sonication)

Animal #	Sex	Age (yrs)	Weight (kg)	# Treatments	Sonication Scheme	Microbubble Doses per Treatment Session*	# Foci Sonicated per Treatment Session*	Neurological Testing	Other Adverse Events	6E10 (Treated/Control)	IBA-1 (Treated/Control)	Prussian Blue (Treated/Control)
1	M	9	12	1	A	6	49	normal	none	4.8/9.3	39.1/27.9	0/0
2	M	10	12.5	1	B	12	50	normal	none	30.3/28.9	37.4/33.2	0/0
3	M	11	11.7	1	B	9	36	normal	none	5.1/5.1	52.7/51.3	2/1
4	F	10	10.1	1	B	12	48	normal	none	0.0/0.6	40.0/50.4	0/0
5	F	10	12.1	1	B	13	52	normal	none	26.4/51.3	36.8/35.8	3/1
6	F	11	12	4	B	11/9/9/9	44/34/34/36	normal	vomiting/ bloody urine	18.1/31.0	24.8/22.4	3/2
7	F	11	13.8	4	B	10/9/8/9	40/35/31/35	normal	none	23.0/2.5	19.6/17.6	7/6
8	F	10	10.6	4	B	8/7/8/7	30/28/32/27	normal	none	22.4/26.5	29.5/31.0	4/2
9	F	10	12.8	4	B	8/8/12/8	31/32/48/31	normal	none	37.9/26.4	36.6/30.9	5/4
10	M	11	12.1	4	B	8/12/8/7	31/46/32/28	normal	none	24.8/44.3	23.4/27.3	7/6

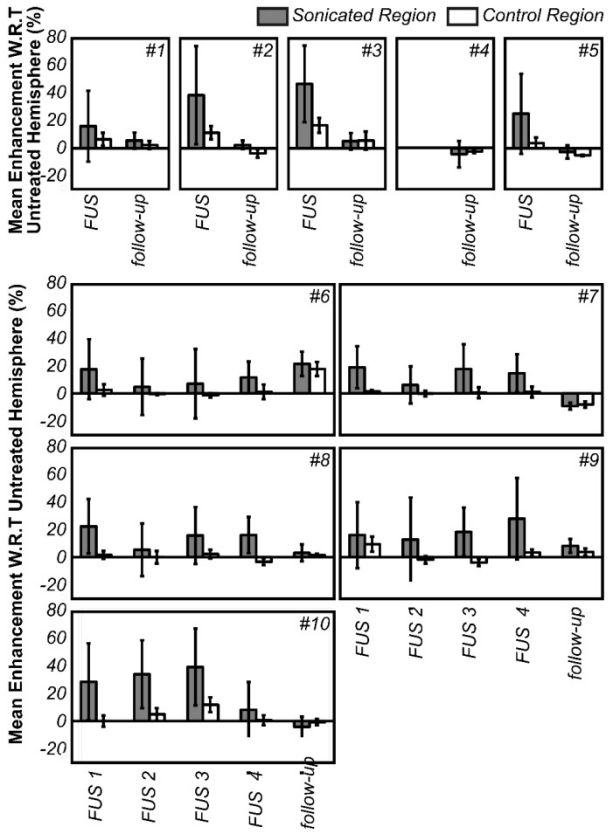

Fig.5. Mean enhancement of the treated hemisphere with respect to the contralateral hemisphere for all animals, expressed as (1-mean_intensity$_{treated}$/ mean_intensity$_{untreated}$)*100%. The enhancement values are averaged over the entire hemisphere. A control (unsonicated) region in the treated hemisphere is also shown (compared to the same contralateral, untreated region) to eliminate bias from spatial sensitivity of the MRI coil. The error bars indicate one standard deviation.

Discussion

This study presents the first investigation of BBB opening in a natural model of aging, and used a large-volume treatment scheme at low, skull penetrating frequency relevant to AD. These results show that after a total of 920 sonications, transient increase in the permeability of the BBB in a whole hemisphere is well tolerated in the aged brain following both single and repeated treatments without any MRI or histological observation of brain damage. One minor adverse event was observed, from which the animal fully recovered and could be attributable to effects from the anesthetic and/or MRI contrast agent. Preliminary histological evidence suggests that ultrasound treatments in a natural disease model is safe and in 3/5 of our animals, particularly in the repeated treatment condition, may also impact plaque pathology as has been seen in transgenic mouse models of AD [18, 19]. In this natural model of aging the amount of plaque pathology varied to a greater degree between animals than the transgenic models, where similar levels of burden are seen for animals of a given age. This canine model is therefore more representative of the clinical scenario, where patients present with varying levels of disease. Additionally, in this study the animals had a range of underlying pathology and it is possible that these pathologies may have interfered with the treatment outcomes. However, this is also more representative of what can be expected clinically, where older patients may have co-morbidities. Unfortunately this also means that a much larger group size would be needed to observe statistically significant changes in plaque load due to treatment.

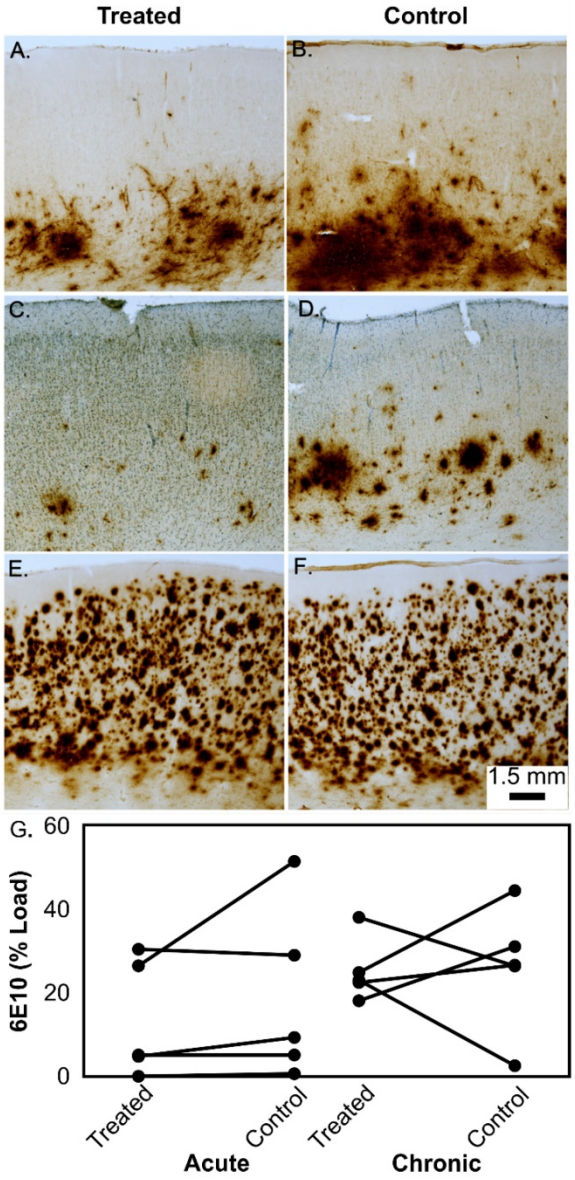

Fig.6. Representative examples of Aβ (6E10) immunostaining in the prefrontal cortex of aged beagles in response to treatment. In a single treatment, the left treated hemisphere shows less Aβ deposition (A) than the right untreated hemisphere (B). Similarly, the left hemisphere of a dog given 4 treatments (C) shows less Aβ than the right untreated hemisphere (D). In contrast, some dogs with significant Aβ neuropathology do not show hemisphere treatment effect (E – single treatment) and right untreated hemisphere (F). Panels A-F all have the same magnification and the scale bar is 1.5 mm. The quantification of the Aβ load is shown in panel (G) for the acute and chronic treatment groups.

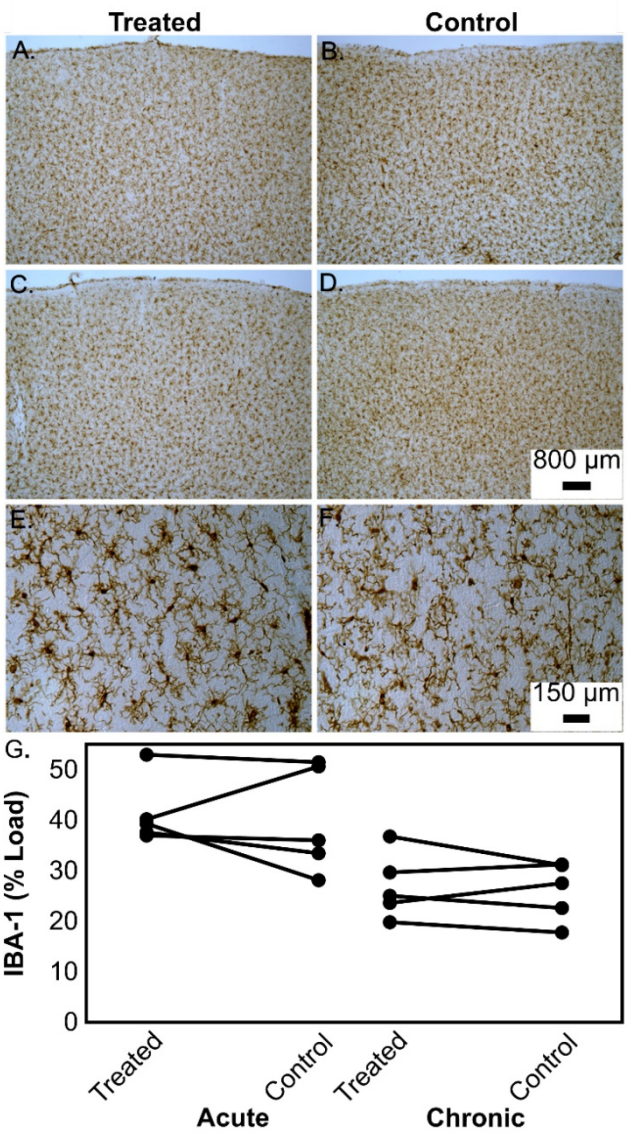

Fig.7. Representative examples of microglial (IBA-1) immunostaining in the prefrontal cortex of aged beagles in response to treatment. In a single treatment, the left treated hemisphere shows similar microglial "loads" (A) to the right untreated hemisphere (B). Similarly, the left hemisphere of a dog given 4 treatments (C) shows similar microglial "loads" to the right untreated hemisphere (D). Panels A-D all have the same magnification and the scale bar is 800 µm. Higher magnification (scale bar 150 µm) of sections from a dog given 4 treatments highlights the morphology of the microglial cells in the left prefrontal cortex (E) as compared to the right prefrontal cortex (F). The quantification of the microglial loads is shown in panel (G) for the acute and chronic treatment groups.

The time course in this study is not ideal for detecting changes in microglia activation, based on work in transgenic mice showing that acutely (4 days) IBA-1 staining is enhanced, but that this effect does not persist to 15 days [17]. As the primary goal of this study was to assess safety, a follow-up period to monitor the animals was necessary, making it impossible to examine the acute microglial response given the small number of subjects available. Thus we decided to measure chronic microglial activation as a possible outcome from the ultrasound treatments, and found that in this natural model the results are in agreement with work in transgenic rodents where a sustained microglial response is not observed.

In this study we used a single element focused transducer operating at a sufficiently low frequency to allow transcranial treatment without having to correct for phase distortions caused by the bone. In this canine model, the parietal bone is relatively flat and the animal can be positioned such that the sound has almost normal incidence to the bone, allowing this simple treatment platform to be used. However, the length of the focal zone for this transducer is long (~40mm) increasing the risk of non-negligible reflections from the skull base. In addition the large focal volume means that the exposure is controlled to the location receiving the highest exposure and the tissue heterogeneity in the focal volume is not compensated for. This can be seen in the variability of the contrast enhancement throughout the sonicated hemisphere. Further the mechanical scanning approach is relatively slow. In future studies, a large aperture phased array transducer that can electronically steer a tighter focal volume around the field would allow for faster treatments with better spatial control of the BBB opening [33].

Although comprehensive studies following repeated, small volume BBB opening in healthy non-human primates [12, 13] have been reported, these canine studies provide important insight into the safety of this treatment in aged dogs with significant Aβ neuropathology. Further, the disruption volume was much larger than has been reported before and was well tolerated, as was the use of multiple microbubble injections (up to 13) per treatment. A previous study in a porcine model tested multiple injections of bubbles at a reduced dose (0.002 ml/kg) to allow up to 10 sonications to be performed while remaining within the recommended maximum dose limit [34], however our study suggests that even higher bubble doses may be safe for treatments requiring serial sonications, as evidenced by our successful use of up to 13 bubble injections at a dose of 0.2 ml/kg per injection. These results suggest that ultrasound opening of the BBB in the aged brain may be a safe treatment option but these preliminary data also suggest the greatest benefit may be in middle-aged dogs prior to Aβ accumulation. Further studies are needed to determine if FUS has a positive impact on naturally occurring Aβ pathology. A larger beneficial effect might also be achieved in future studies by combining the FUS opening of the BBB with the delivery of a therapeutic, such as an Aβ antibody [6], if FUS alone cannot produce a therapeutically relevant effect.

In addition to the small group size, another limitation is that this study did not include a sham treatment group as a control for the behavior testing or histological analysis. However, the individuals performing the behavior analysis were blinded to the treatment hemisphere and the degree of BBB opening (as determined by MRI enhancement) achieved during treatment. Further, based on prior studies in aged beagles that have not undergone ultrasound treatments, it has been found that old dogs can have widely varying Aβ loads [35, 36]. However, to our knowledge, there are no studies directly comparing Aβ deposition in the left and right hemispheres of aging dogs, thus in future studies, it will be critical to include sham treated animals.

Clinical Translation: A commercial device already exists that would allow this technique to be implemented in the clinic, and this device has previously been tested in a healthy, large animal model [34]. While the ultrasound frequency used in this study is comparable to the commercial device, some of the other study parameters may need to be adjusted to be used in clinic. As discussed above, the total dose of microbubbles/treatment was higher in this study than the clinically recommended limit. Although our study suggests that in the future a higher total bubble dose, given over multiple injections, could be safe, initially lower bubble doses will most likely be used, similar to the scheme described by [34]. During the repeated treatments we limited the total number of MR contrast agent injections to 2, following an adverse reaction. Similarly, in the clinical setting it would be important to limit the total dose of MR contrast. Finally, in our study we used an active control scheme to ensure a safe ultrasound exposure level. This controller is currently not implemented in an automated fashion on the commercial device, but a similar approach could be manually implemented by increasing exposures until the desired bubble behavior is observed by the operator. This study demonstrates the safety of this approach in a clinically-relevant disease model with large treatment volumes and paves the way for clinical testing in AD patients in the very near future.

Acknowledgments

Support for this work was provided by the W. Garfield Weston Foundation, the Canadian Institutes for Health Research (FRN 119312), the National Institute of Biomedical Imaging and Bioengineering of the National Institutes of Health (R01 EB003268) and the Canada Research Chair Program. The authors would like to thank Shawna Rideout, Alexandra Garces, Linda Ngheim and Angela Chow for their help with the animal care and the collection of the behavioural data. The authors would also like to thank Dr. Yuexi Huang for his assistance with the CT imaging, Lucy Deng for experimental assistance, and Sylvia Lam, My-Linh Yee and Olivia Hough for their assistance with data processing.

Competing Interests

KH and MAO are listed as co-inventors on a patent application related to the ultrasound methods used in this study. KH is an inventor in patents owned by Sunnybrook Research Institute and Brigham and Women's Hospital. KH owns stock in FUS Instruments that has licensed this IP for preclinical use. The other authors have no conflicts to declare.

References

[1] Pardridge WM. The blood-brain barrier: bottleneck in brain drug development. NeuroRx. 2005;2(1):3–14.
[2] Hynynen K, McDannold N, Vykhodtseva N, Jolesz FA. Noninvasive MR imaging-guided focal opening of the blood-brain barrier in rabbits. Radiology. 2001;220(3):640–646.
[3] Liu HL, Hua MY, Chen PY, Chu PC, Pan CH, Yang HW, et al. Blood-brain barrier disruption with focused ultrasound enhances delivery of chemotherapeutic drugs for glioblastoma treatment. Radiology. 2010;255(2):415–425.
[4] Treat LH, McDannold N, Vykhodtseva N, Zhang Y, Tam K, Hynynen K. Targeted delivery of doxorubicin to the rat brain at therapeutic levels using MRI-guided focused ultrasound. Int J Cancer. 2007;121(4):901–907.
[5] Aryal M, Vykhodtseva N, Zhang YZ, Park J, McDannold N. Multiple treatments with liposomal doxorubicin and ultrasound-induced disruption of blood-tumor and blood-brain barriers improve outcomes in a rat glioma model. J Controlled Release. 2013;169(1-2):103–111.
[6] Jordão JF, Ayala-Grosso CA, Markham K, Huang Y, Chopra R, McLaurin J, et al. Antibodies targeted to the brain with image-guided focused ultrasound reduces amyloid-beta plaque load in the TgCRND8 mouse model of Alzheimer's disease. PLoS ONE. 2010;5(5):e10549.
[7] Kinoshita M, McDannold N, Jolesz FA, Hynynen K. Noninvasive localized delivery of Herceptin to the mouse brain by MRI-guided focused ultrasound-induced blood-brain barrier disruption. Proc Natl Acad Sci U S A. 2006;103(31):11719–11723.
[8] Huang Q, Deng J, Wang F, Chen S, Liu Y, Wang Z, et al. Targeted gene delivery to the mouse brain by MRI-guided focused ultrasound-induced blood-brain barrier disruption. Exp Neurol. 2012;233(1):350–356.
[9] Thévenot E, Jordão JF, O'Reilly MA, Markham K, Weng YQ, Foust KD, et al. Targeted delivery of self-complementary adeno-associated virus serotype 9 to the brain, using magnetic resonance imaging-guided focused ultrasound. Hum Gene Ther. 2012;23(11):1144–1155.
[10] Alonso A, Reinz E, Leuchs B, Kleinschmidt J, Fatar M, Geers B, et al. Focal Delivery of AAV2/1-transgenes Into the Rat Brain by Localized Ultrasound-induced BBB Opening. Mol Ther Nucleic Acids. 2013;2:e73.
[11] Burgess A, Ayala-Grosso CA, Ganguly M, Jordão JF, Aubert I, Hynynen K. Targeted delivery of neural stem cells to the brain using MRI-guided focused ultrasound to disrupt the blood-brain barrier. PLoS One. 2011;6(11):e27877.
[12] McDannold N, Arvanitis CD, Vykhodtseva N, Livingstone MS. Temporary disruption of the blood-brain barrier by use of ultrasound and microbubbles: safety and efficacy evaluation in rhesus macaques. Cancer Res. 2012;72(14):3652–3663.
[13] Downs ME, Buch A, Sierra C, Karakatsani ME, Teichert T, Chen S, et al. Long-Term Safety of Repeated Blood-Brain Barrier Opening via Focused Ultrasound with Microbubbles in Non-Human Primates Performing a Cognitive Task. PLoS One. 2015;10(5):e0125911.
[14] Horodyckid C, Canney M, Vignot A, Boisgard R, Drier A, Huberfeld G, et al. Safe long-term repeated disruption of the blood-brain barrier using an implantable ultrasound device: a multiparametric study in a primate model. J Neurosurg. 2016;:1–11.
[15] Carpentier A, Canney M, Vignot A, Reina V, Beccaria K, Horodyckid C, et al. Clinical trial of blood-brain barrier disruption by pulsed ultrasound. Sci Transl Med. 2016;8(343):343re2.
[16] Huang Y, Alkins R, Chapman M, Perry J, Sahgal A, Trudeau M, et al. Initial experience in a pilot study of blood-brain barrier opening for chemo-drug delivery to brain tumors by MR-guided focused ultrasound. In: 24th Annual Meeting of the International Society for Magnetic Resonance in Medicine; 2016. .

[17] Jordão JF, Thévenot E, Markham-Coultes K, Scarcelli T, Weng YQ, Xhima K, et al. Amyloid-β plaque reduction, endogenous antibody delivery and glial activation by brain-targeted, transcranial focused ultrasound. Exp Neurol. 2013;248:16–29.
[18] Burgess A, Dubey S, Yeung S, Hough O, Eterman N, Aubert I, et al. Alzheimer disease in a mouse model: MR imaging-guided focused ultrasound targeted to the hippocampus opens the blood-brain barrier and improves pathologic abnormalities and behavior. Radiology. 2014;273(3):736–745.
[19] Leinenga G, Götz J. Scanning ultrasound removes amyloid-β and restores memory in an Alzheimer's disease mouse model. Sci Transl Med. 2015;7(278):278ra33.
[20] Elder GA, Gama Sosa MA, De Gasperi R. Transgenic mouse models of Alzheimer's disease. Mt Sinai J Med. 2010;77(1):69–81.
[21] Cotman CW, Head E. The canine (dog) model of human aging and disease: dietary, environmental and immunotherapy approaches. J Alzheimers Dis. 2008;15(4):685–707.
[22] O'Reilly MA, Huang Y, Hynynen K. The impact of standing wave effects on transcranial focused ultrasound disruption of the blood-brain barrier in a rat model. Phys Med Biol. 2010;55:5251–5267.
[23] Ellens NPK, Kobelevskiy I, Chau A, Waspe AC, Staruch RM, Chopra R, et al. The targeting accuracy of a preclinical MRI-guided focused ultrasound system. Med Phys. 2015;42(1):430–439.
[24] O'Reilly MA, Hynynen K. Ultrasound enhanced drug delivery to the brain and central nervous system. Int J Hyperthermia. 2012;28(4):386–396.
[25] O'Reilly MA, Hynynen K. A PVDF receiver for ultrasound monitoring of transcranial focused ultrasound therapy. IEEE Trans Biomed Eng. 2010;57(9):2286–2294.
[26] Clement GT, White PJ, Hynynen K. Enhanced ultrasound transmission through the human skull using shear mode conversion. J Acoust Soc Am. 2004;115:1356–1364.
[27] White PJ, Clement GT, Hynynen K. Longitudinal and shear mode ultrasound propagation in human skull bone. Ultrasound Med Biol. 2006;32:1085–1096.
[28] Karakatsani MEM, Samiotaki GM, Downs ME, Ferrera VP, Konofagou EE. Targeting Effects on the Volume of the Focused Ultrasound-Induced Blood-Brain Barrier Opening in Nonhuman Primates In Vivo. IEEE Trans Ultrason Ferroelectr Freq Control. 2017;64:798–810.
[29] Head E, McCleary R, Hahn FF, Milgram NW, Cotman CW. Region-specific age at onset of beta-amyloid in dogs. Neurobiol Aging. 2000;21(1):89–96.
[30] Head E, Pop V, Vasilevko V, Hill M, Saing T, Sarsoza F, et al. A two-year study with fibrillar beta-amyloid (Abeta) immunization in aged canines: effects on cognitive function and brain Abeta. J Neurosci. 2008;28(14):3555–3566.
[31] Kitamoto T, Ogomori K, Tateishi J, Prusiner SB. Formic acid pretreatment enhances immunostaining of cerebral and systemic amyloids. Lab Invest. 1987;57(2):230–236.
[32] Wilcock DM, Rojiani A, Rosenthal A, Subbarao S, Freeman MJ, Gordon MN, et al. Passive immunotherapy against Abeta in aged APP-transgenic mice reverses cognitive deficits and depletes parenchymal amyloid deposits in spite of increased vascular amyloid and microhemorrhage. J Neuroinflammation. 2004;1(1):24.
[33] Deng L, O'Reilly MA, Jones RM, An R, Hynynen K. A multi-frequency sparse hemispherical ultrasound phased array for microbubble-mediated transcranial therapy and simultaneous cavitation mapping. Phys Med Biol. 2016;61:8476–8501.
[34] Huang Y, Alkins R, Schwartz ML, Hynynen K. Opening the Blood-Brain Barrier with MR Imaging-guided Focused Ultrasound: Preclinical Testing on a Trans-Human Skull Porcine Model. Radiology. 2017;282:123–130.
[35] Cummings BJ, Head E, Afagh AJ, Milgram NW, Cotman CW. Beta-amyloid accumulation correlates with cognitive dysfunction in the aged canine. Neurobiol Learn Mem. 1996;66:11–23.
[36] Head E, Callahan H, Muggenburg BA, Cotman CW, Milgram NW. Visual-discrimination learning ability and beta-amyloid accumulation in the dog. Neurobiol Aging. 1998;19:415–425.